

Electronic Supplementary Information for

Ionochemical synthesis of sulfur-doped porous carbons hybridized with graphene as superior anode materials for lithium-ion batteries

Yang Yan, Ya-Xia Yin, Sen Xin, Yu-Guo Guo* and Li-Jun Wan*

Key Laboratory of Molecular Nanostructure and Nanotechnology, and Beijing National Laboratory for Molecular Sciences (BNLMS), Institute of Chemistry, Chinese Academy of Sciences (CAS), Beijing, 100190, P. R. China

*Correspondence author. E-mail: yguo@iccas.ac.cn; wanlijun@iccas.ac.cn

Experimental Section

Synthesis of SPC@G nanocomposite: Graphite oxide was synthesized from natural graphite by a modified Hummer's method.¹

In a typical synthesis, 50 mg graphite oxide was firstly ultrasonicated in 10mL de-ionized water for 1h. Then, 10 mL [BMIM] [HSO₄] and 1 g D-glucose were added to the aqueous GO suspension under sonication for 1h. The mixtures of IL/H₂O/GO/glucose were distilled using a rotary evaporator for 10 h under vacuum at 80 °C. The resulting suspension was transferred to a 25mL Teflon autoclave, which was then heated at 180 °C for 12h. A gelatinous product was harvested and washed with DI water several times. After dried in an oven at 80 °C, the precursor was annealed to obtain the SPC@graphene at 800 °C for 2h in Ar atmosphere with a heating rate of 5 °C /min. Also, for preparing the control materials of the SPC or rGO, the SPC or rGO precursor was prepared under the same condition without adding the GO or D-glucose during the ultrasonication process.

Structural Characterization: The morphology of the final products was observed by SEM (JEOL 6701F, operating at 10kV), TEM and HRTEM (Tecnai F20 operating at 200 kV). X-ray diffraction (XRD) measurement was carried out using a Rigaku D/max2500 diffractometer with filtered Cu K α radiation. Raman spectra were obtained using a Digilab FTS3500 from Bio-Rad with a laser wavelength of 632.8 nm. Nitrogen adsorption and desorption isothermal at 77.3 K were performed with Nova 2000e surface area-pore size analyzer. XPS analysis was conducted on an ESCALab220i-XL electron spectrometer from VG Scientific using 300W Al K α radiation.

Electrochemical Measurements: Electrochemical measurements were carried out by using Swagelok-type cells assembled in an argon-filled glovebox. For preparing

working electrodes, a mixture of active material, super-P acetylene black, and poly(vinyl difluoride) (PVDF) at a weight ratio of 80:10:10 was pasted on a Cu foil. Pure lithium foil was used as a counter electrode. Both positive and negative electrodes were separated by a Whatman GF/D glass-fiber. The electrolyte consist of a solution of 1 M LiPF₆ in ethylene carbonate (EC)/dimethyl carbonat (DMC)/diethyl carbonate (DEC) with a weight ratio of 1:1:1 obtained from Tianjin Jinniu Power Sources Material Co. Ltd. Cyclic voltammetry (CV) and Electrochemical impedance spectral (EIS) measurements were carried out on an Autolab PG203N. Galvanostatic cycling of the cells was performed using an Arbin BT2000 system in the voltage range of 0.01-3 V (vs. Li⁺/Li). The cutoff voltage of 3 V was determined considering the complete charge process for the porous carbon which is consistent with the porous carbon anode materials in other literatures.²⁻⁹

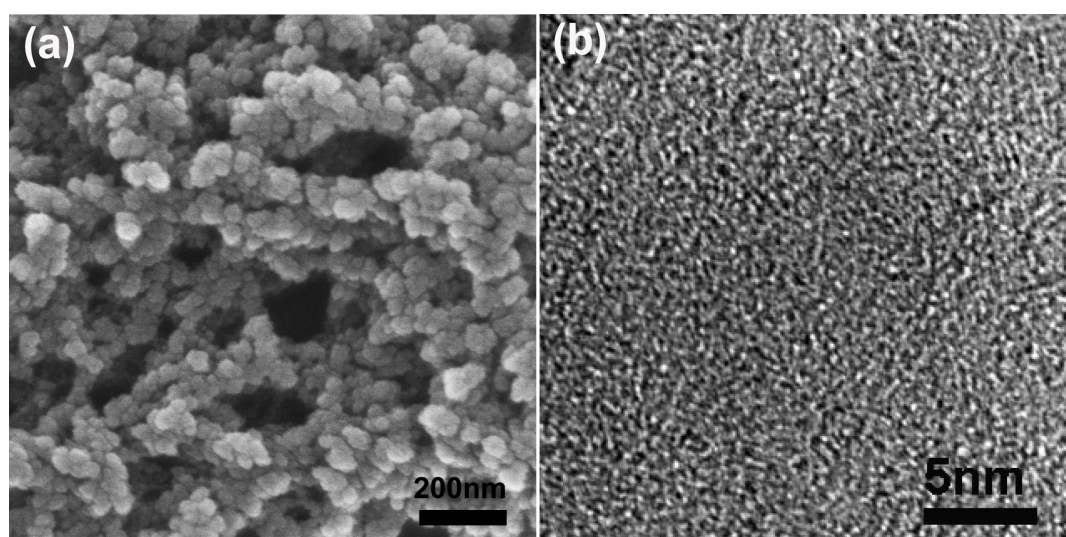


Fig. S1. (a) SEM image and (b) HRTEM image of SPC.

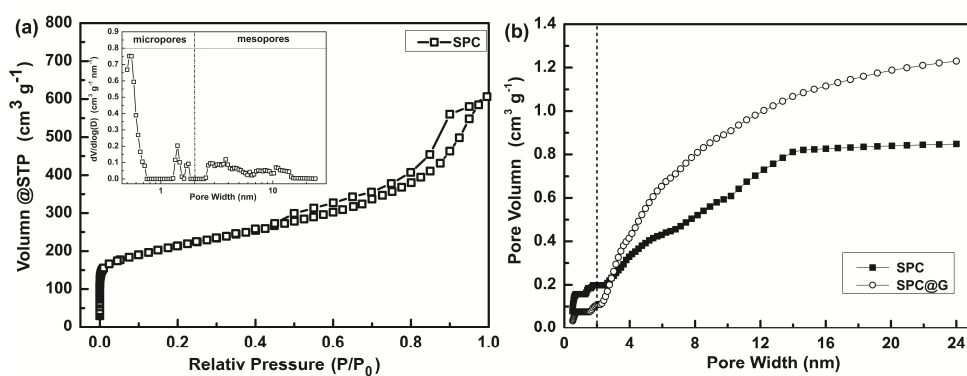


Fig. S2. (a) Nitrogen adsorption/desorption isotherms and corresponding pore-size distribution curve (inset) of SPC and (b) the cumulative pore volume of SPC and SPC@G.

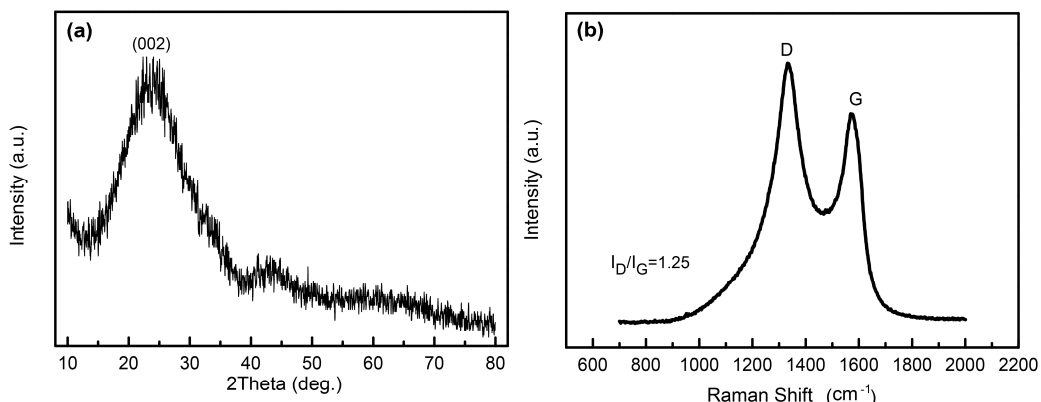


Fig. S3. (a) X-ray diffraction (XRD) pattern and (b) Raman spectrum of the SPC@G nanocomposite. As shown in Fig. S3a, the lattice space is 0.376 nm (calculated by Bragg equation), larger than that of (002) plane for graphite (0.335 nm), which indicates the low graphitization degree of the SPC@G. Moreover, the broad (002) diffraction peak in the XRD pattern confirms the low degree of graphitization. The Raman spectroscopy shows that the two remarkable peaks around 1338 and 1590 cm^{-1} can be attributed to D band arising from the defects and disorders in carbonaceous material and G band associated with the E_{2g} mode of graphite.⁹ The intensity ratio (I_D/I_G) of the two bands is about 1.25, further confirming the low graphitization degree of SPC@G.

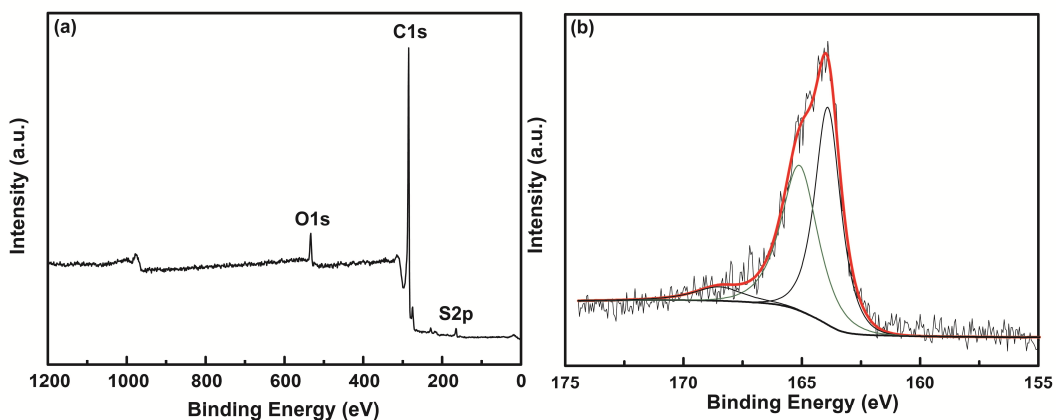


Fig. S4. (a) XPS survey scan and (b) S2p spectra of SPC. Besides C1s and O1s, S2p spectrum is observed in the SPC. The S2p peak of the SPC can be resolved into three peaks at binding energies of ~ 164.0 , 165.2 , and 168.5 eV , which is consistent with the SPC@G. Especially, the sulfur content in the SPC@G is calculated to be 1.88%.

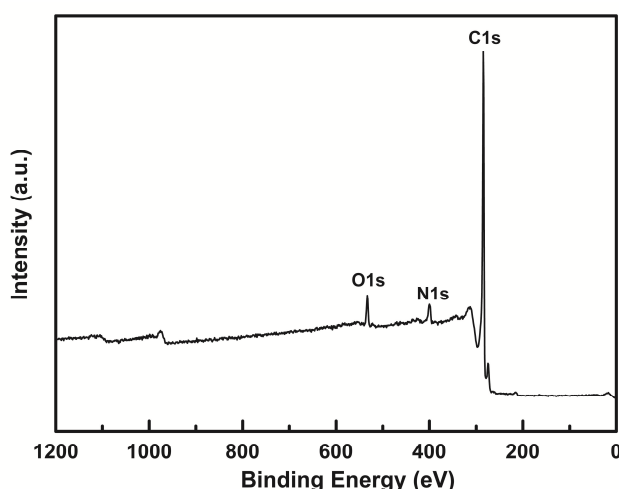


Fig. S5. XPS survey scan of rGO synthesized by the ionothermal process. The survey scan of rGO not only indicates the existence of C and O, but also N, which is coming from the absorption of the Bmim^+ on the surface.

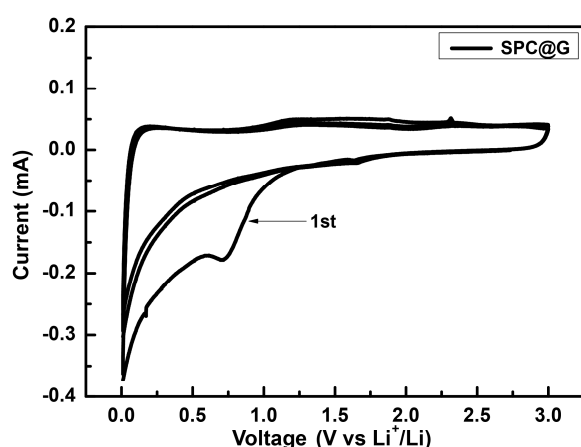


Fig. S6. Cyclic Voltammograms of SPC@G nanocomposite at a scan rate of 0.1 mV s^{-1}

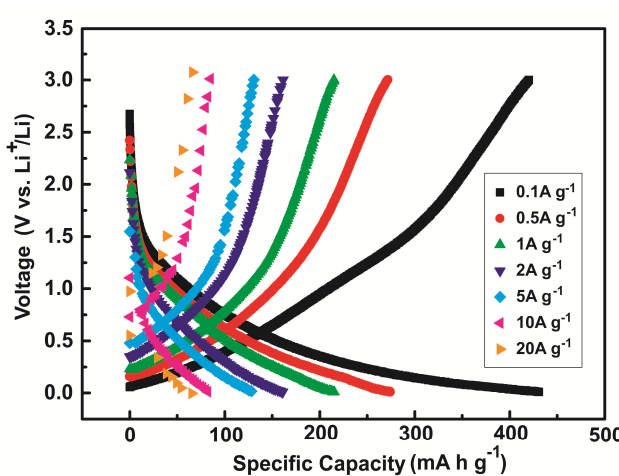


Fig. S7. Galvanostatic discharge/charge curves of rGO under different current densities.

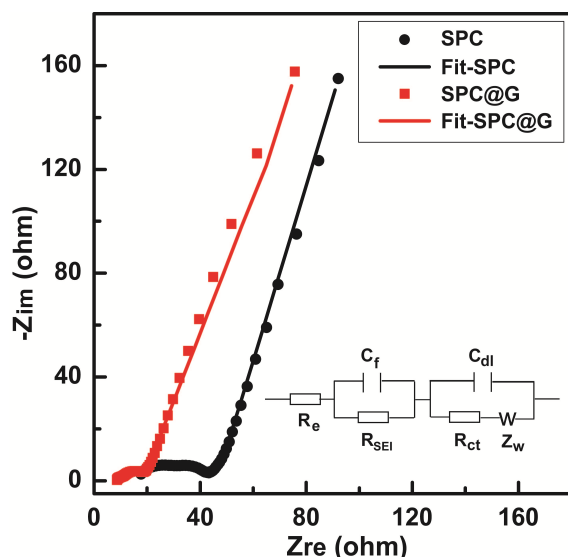


Fig. S8. Nyquist plots after rate performance tests of the graphene-free SPC and the SPC@G nanocomposite. As shown in this Figure, both the Nyquist plots for the SPC and SPC@G exhibit two depressed semicircles and an inclined line, similar to non-graphite carbonaceous materials. The equivalent circuit (inset of Fig. S8) was adopted to further clarify the meaning of the semicircles and the inclined line. The total resistance of electrolyte R_e , the resistance of the SEI film R_{SEI} and the charge-transfer resistance R_{ct} all contributes to the semicircle, while Z_W is the Warburg impedance arising from the lithium-diffusion process within carbon electrodes.^{3, 9, 10} Obviously, the R_{SEI} and R_{ct} for the SPC@G nanocomposite is 2.49 and 7.31 Ω , respectively, which is lower than that of the graphene-free SPC (13.27 and 9.91 Ω).

References

1. W. S. Hummers and R. E. Offeman, *J. Am. Chem. Soc.*, 1958, **80**, 1339-1339.
2. Y. S. Hu, P. Adelhelm, B. M. Smarsly, S. Hore, M. Antonietti and J. Maier, *Adv. Funct. Mater.*, 2007, **17**, 1873-1878.
3. S. Yang, X. Feng, L. Zhi, Q. Cao, J. Maier and K. Müllen, *Adv. Mater.*, 2010, **22**, 838-842.
4. S. Yang, L. Zhi, K. Tang, X. Feng, J. Maier and K. Müllen, *Adv. Funct. Mater.*, 2012, 1-7.
5. L. Qie, W.-M. Chen, Z.-H. Wang, Q.-G. Shao, X. Li, L.-X. Yuan, X.-L. Hu, W.-X. Zhang and Y.-H. Huang, *Adv. Mater.*, 2012, **24**, 2047-2050.
6. H. Wang, C. Zhang, Z. Liu, L. Wang, P. Han, H. Xu, K. Zhang, S. Dong, J. Yao and G. Cui, *J. Mater. Chem.*, 2011, **21**, 5430-5434.
7. Z.-S. Wu, W. Ren, L. Xu, F. Li and H.-M. Cheng, *ACS Nano*, 2011, **5**, 5463-5471.
8. S. Ito, T. Murate, M. Hasegawa, Y. Bito and Y. Toyoguchi, *J. Power Sources*, 1997, **68**, 245-248.
9. B. Guo, X. Wang, P. F. Fulvio, M. Chi, S. M. Mahurin, X.-G. Sun and S. Dai, *Adv. Mater.*, 2011, **23**, 4661-4666.
10. X. Sun and C. A. Angell, *Electrochim. Commun.*, 2009, **11**, 1418-1421.